Journal of Medicinal Chemistry

Article

pubs.acs.org/jmc

Novel Cytidine-Based Orotidine-5′-Monophosphate Decarboxylase Inhibitors with an Unusual Twist

Meena K. Purohit,[†,‡] Ewa Poduch,[†] Lianhu William Wei,[†] Ian Edward Crandall,[§] Terrence To,[⊥] Kevin C. Kain,[#,▽] Emil F. Pai,[§,⊥,∥] and Lakshmi P. Kotra*[,†,‡,§,▽]

[†]Center for Molecular Design and Preformulations, Toronto General Research Institute, University Health Network, Toronto, Ontario M5G 1L7, Canada

[‡]Department of Pharmacy, Birla Institute of Technology and Science, Pilani, Rajasthan, India

[§]Department of Pharmaceutical Sciences, Leslie Dan Faculty of Pharmacy, University of Toronto, 144 College Street, Toronto, Ontario M5S 3M2, Canada

[⊥]Campbell Family Cancer Research Institute, Ontario Cancer Institute, 610 University Avenue, Toronto, Ontario M5G 2M9, Canada

[∥]Departments of Medical Biophysics, Biochemistry, and Molecular Genetics, University of Toronto, 1 King's College Circle, Toronto, Ontario M5S 1A8, Canada

[#]Tropical Disease Unit, Division of Infectious Diseases, Department of Medicine, UHN-Toronto General Hospital and the University of Toronto and McLaughlin-Rotman Center/UHN, University of Toronto, Toronto, Ontario, Canada

[▽]McLaughlin Center for Molecular Medicine, University of Toronto, Toronto, Ontario, Canada

Supporting Information

ABSTRACT: Orotidine-5′-monophosphate decarboxylase (ODCase) is an interesting enzyme with an unusual catalytic activity and a potential drug target in *Plasmodium falciparum*, which causes malaria. ODCase has been shown to exhibit unusual and interesting interactions with a variety of nucleotide ligands. Cytidine-5′-monophosphate (CMP) is a poor ligand of ODCase, and CMP binds to the active site of ODCase with an unusual orientation and conformation. We designed N3- and N4-modified CMP derivatives as novel ligands to ODCase. These novel CMP derivatives and their corresponding nucleosides were evaluated against *Plasmodium falciparum* ODCase and parasitic cultures, respectively. These derivatives exhibited improved inhibition of the enzyme catalytic activity, displayed interesting binding conformations and unusual molecular rearrangements of the ligands. These findings with the modified CMP nucleotides underscored the potential of transformation of poor ligands to ODCase into novel inhibitors of this drug target.

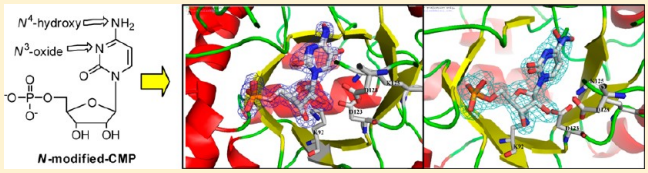

INTRODUCTION

Orotidine-5′-monophosphate decarboxylase (ODCase, EC 4.1.1.23) catalyzes the decarboxylation of orotidine-5′-monophosphate (OMP, **2**) to uridine-5′-monophosphate (UMP, **1**) during *de novo* pyrimidine biosynthesis. Pyrimidine nucleotides are necessary for the biological construction of DNA and RNA. The catalytic activity of ODCase does not involve any cofactors, metal ions, or intermittent covalent bond formation. The half-time ($t_{1/2}$) for the uncatalyzed decarboxylation reaction of **2** is about 78 million years, but when catalyzed by ODCase, it is 18 ms.[1,2] ODCase is present in most living organisms including humans, bacteria, and various parasites. Due to the significant physiological role of ODCase in living organisms, this proficient enzyme could be a valuable drug target if compounds can be designed to selectively inhibit pathogen enzymes.[3] Several known C-6 substituted nucleoside inhibitors of ODCase exhibit potent antimalarial activities (Chart 1).[4] Recent discoveries of fluorinated nucleosides as ODCase inhibitors that exhibit anticancer and antiviral activities also demonstrate its potential for inhibitor development.[5,6] These investigations provided insights into the biochemical nature of this enzyme, binding conformations of various ligands

Chart 1. Structures of ODCase Substrate 2 and Various Known Inhibitors

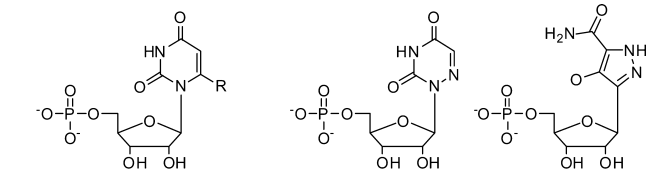

1, R = H (UMP) **2**, R = COOH (OMP) **9** (6-aza UMP) **10** (Pyrazofurin)
3, R = OH (BMP) **4**, R = CN
5, R = I **6**, R = N_3
7, R = NH_2 **8**, R = CH_3

Received: August 9, 2012
Published: September 19, 2012

in its active site, and binding of inhibitors to this therapeutic target.

Thus, ODCase has captivated biochemists for the last three decades. To date, 152 crystal structures of ODCase and its complexes from both prokaryotic and eukaryotic organisms have been solved and appear in the Protein Data Bank.[7] Still after a significant number of mechanistic studies and three-dimensional structure elucidations, the underlying chemical mechanism for its catalytic biochemical activity remains unclear. However, the active site of the enzyme has been very well mapped.

The active site of ODCase is fairly small and rigid, with four conserved catalytic amino acid residues, Lys42, Asp70, Lys72, and Asp75[B], in its center.[8] Despite the restricted environment, both pyrimidine- and purine-based nucleotides fit in the ODCase active site exposing its plasticity.[9,10] ODCase is naturally evolved to bind to nucleotides carrying uracil-type nucleobases, considering its dedicated function in the cell for the decarboxylation of **2** to yield **1**. Additionally, the binding conformation of **1** in the enzymatic pocket of ODCase gives insight into the types of preferable interactions and binding positions within the active site. It has been reported that the nucleobase of cytidine-5′-monophosphate (CMP) binds to the active site of ODCase in a mode different from that of **1**. In this binding mode, the phosphate and ribosyl moieties sit in a similar fashion as found for **1**, but the pyrimidine assumes a completely different orientation as well as conformation, almost reaching outside of the binding pocket.[11,12] Due to its unusual binding conformation in the active site of ODCase, CMP (**11**) fails to undergo optimum interactions and is thus unable to effectively inhibit the catalytic site. This is further demonstrated by the difference in K_i values between **1** and CMP for the inhibition of *Hs*ODCase (220 ± 10 and 1200 ± 700 μM, respectively).[9]

N-Modified CMP derivatives, especially at the N3 and N4 positions of CMP, were conceived as novel ligands to ODCase (Chart 2), with the anticipation to create novel interactions for

Chart 2. Design of Unusual CMP Analogs

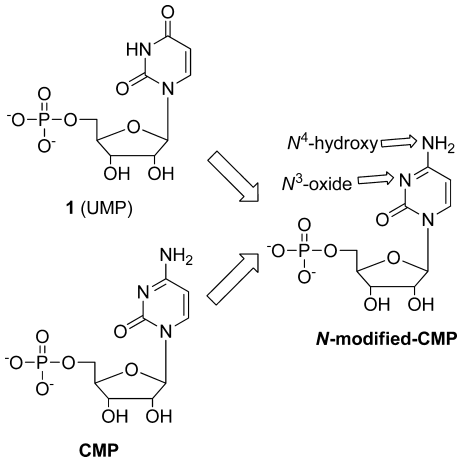

the CMP ligands in the ODCase binding site, as well as to improve on its affinity. Thus, N3 and N4 oxygen-substituted cytidine-based derivatives were synthesized and screened for their inhibition of ODCases. Here, we disclose the chemistry and biochemistry of N3- and N4-substituted CMP derivatives in the context of the therapeutic target, ODCase.

EXPERIMENTAL SECTION

General. All solvents and reagents were obtained from commercial sources. Column chromatography purifications were performed on Biotage flash chromatography systems using normal silica gel (60 Å, 70−230 mesh) and reverse-phase (C18) cartridges. Reactions were monitored by thin layer chromatography (Merck). NMR spectra were recorded on Bruker spectrometers (400 MHz for ^{1}H and 162.03 MHz for ^{31}P). Chemical shifts are reported in δ ppm using the residual solvent peak as the reference for the ^{1}H NMR spectra, and phosphoric acid as external standard for the ^{31}P spectrum. Purity of the synthesized compounds was determined by a Waters HPLC system (Delta 600) or LC-MS system (Waters 2545 binary gradient module). Mass spectra (ESI) were recorded on a Waters LC/MS system equipped with a Waters 3100 mass detector. HPLC methodology was used to determine purity of the final compounds, and their purity is ≥95%. All enzyme assays were performed at either 37 or 55 °C using a VP-ITC microcalorimeter (MicroCal, Northampton, MA) according to previously published procedures.[13] The pH of the buffers was measured with a Corning 430 pH meter.

Synthesis. *4-Amino-1-(3,4-dihydroxy-5-hydroxymethyl-tetrahydrofuran-2-yl)-1H-pyrimidin-2-one-3-oxide (Cyd-N^3-oxide, **13**).* Cytidine (100 mg, 0.41 mmol) was suspended in anhydrous methanol (4 mL). *m*-Chloroperbenzoic acid (213 mg, 1.23 mmol) was added in fractions to the reaction suspension at 0 °C. The reaction mixture was allowed to stir at 0 °C for 15 min. After 24 h of stirring at room temperature, the reaction solvent was evaporated to dryness. Water (4 mL) was added to precipitate *m*-chlorobenzoic acid. The byproduct was filtered off, and the filtrate was purified by reverse phase chromatography on HPLC (Supporting Information). Fractions containing the compound of interest were mixed together and lyophilized to give compound **13** as a white solid (62 mg, 58%). ^{1}H NMR (D_2O) δ 3.85 (dd, J = 12, 44 Hz, 2H, 5′ and 5″), 4.13−4.19 (m, 2H, 4′ and 3′), 4.35 (dd, J = 3.36, 1.16 Hz, 1H, 2′), 5.87 (d, J = 3.24 Hz, 1H, 1′), 6.31 (d, J = 8.00 Hz, 1H, 5), 8.04 (d, J = 8.04 Hz, 1H, 6). ESI (+) m/z calcd for $C_9H_{13}N_3O_6$ [M + H$^+$] 260.09, found 260.11 Da.

*(5-(4-Amino-3-oxido-2-oxopyrimidin-1-yl)-3,4-dihydroxyoxolan-2-yl)-methyl Dihydrogen Phosphate (CMP-N^3-oxide, **14**).* Compound **14** was synthesized similar to compound **13** from CMP (100 mg, 0.27 mmol). The product was purified by HPLC using a reverse phase semipreparatory column (Supporting Information). Fractions containing the desired compound were collected and lyophilized. The free acid form of compound **14** was neutralized by NH_4OH to yield the ammonium salt of CMP-N^3-oxide (48 mg, 42%). ^{1}H NMR (D_2O) δ 4.04 (dd, J = 12.24, 37.16 Hz, 2H, 5′ and 5″), 4.26 (m, 1H, 4′), 4.30−4.36 (m, 2H, 3′and 2′), 5.98 (d, J = 2.6 Hz, 1H, 1′), 6.36 (d, J = 7.84 Hz, 5), 8.10 (d, J = 7.6 Hz, 6). ^{31}P (D_2O) δ −3.647. ESI (−) m/z calcd for $C_9H_{14}N_3O_9P$[M − H$^+$] 339.05, found 338.21 Da.

*1-(3,4-Dihydroxy-5-(hydroxymethyl)tetrahydrofuran-2-yl)-4-(hydroxyamino)pyrimidin-2[1H]-one (N^4-OH-Cyd, **15**).* Hydroxyl ammonium acetate[14] was synthesized by adjusting the pH of 5 N NH_2OH with acetic acid to 5.98. Cytidine (50 mg, 0.20 mmol) was dissolved in 2.5 mL of hydroxyl ammonium acetate at room temperature. The reaction mixture was then warmed to 37 °C and stirred for 15 h. The reaction solvent was evaporated, and the reaction crude was dissolved in 2 mL of water. It was then purified by reverse phase chromatography on HPLC (Supporting Information). Aqueous fractions containing the target compound were collected and lyophilized to yield compound **15** (32 mg, 60%). ^{1}H NMR (D_2O) δ 3.85 (dd, J = 12, 44 Hz, 2H, 5′and 5″), 4.07 (br m, 1H, 4′), 4.18 (br dd, J = 4.68, 5.40 Hz, 1H, 3′), 4.29 (br dd, J = 5.28, 5.00 Hz, 1H, 2′), 5.84−5.86 (m, 2H, 1′ and 5), 7.34 (d, J = 8.28 Hz, 1H, 6). ESI (+) m/z calcd for $C_9H_{13}N_3O_6$[M + H$^+$] 260.09, found 260.11 Da.

*4-Amino-1-(6-(hydroxymethyl)-2,2-dimethyltetrahydrofuro[3,4-d][1,3]dioxol-4-yl)pyrimidin-2[1H]-one (**24**).* In a flame-dried flask, a suspension of cytidine (500 mg, 2.05 mmol) in anhydrous acetone (40 mL) was cooled to 0 °C and treated with conc. H_2SO_4 (0.25 mL) dropwise. After stirring at room temperature for 12 h, the reaction mixture was neutralized by NH_4OH and purified over silica gel (10% MeOH in DCM). Organic fractions containing the compound of interest were evaporated to obtain compound **24** as a white solid (547

dx.doi.org/10.1021/jm301176r | J. Med. Chem. 2012, 55, 9988−9997

mg, 93%). ^{1}H NMR ($CDCl_3$) δ 1.34 (s, 3H, *iso* CH_3), 1.55 (s, 3H, *iso* CH_3) 3.83 (dd, J = 35.42, 11.16 Hz, 2H, 5′ and 5″), 4.30 (br m, 1H, 4′), 4.96 (br m, 1H, 3′), 5.02 (br m,1H, 2′), 5.57 (br s, 1H, 1′), 6.00 (d, J = 7.36 Hz, 1H, 5), 7.57 (d, J = 7.44 Hz, 1H, 6).

*(6-(4-Amino-2-oxopyrimidin-1(2H)-yl)-2,2-dimethyltetrahydrofuro[3,4-d][1,3]dioxol-4-yl)methyl Diethyl Phosphate (**25**).* Compound **24** (547 mg, 1.93 mmol) was dissolved in 2 mL of anhydrous pyridine. The reaction mixture was cooled to 0 °C and diethyl chlorophosphate (333 mg, 1.93 mmol) was added dropwise. The reaction was stirred at 0 °C for 30 min and then for an additional 15 min at room temperature. The reaction was quenched with 2 mL of MeOH and purified over silica gel (10% MeOH in DCM) to give compound **25** as a white solid (479 mg, 67%). ^{1}H NMR ($CDCl_3$) δ 1.25−1.27 (*br*, m, 9H, 3 CH_3), 1.48 (s, 3H, *iso* CH_3), 3.65−4.27 (m, 7H, 5′, 5″, 4′ and *diethyl* $2CH_2$), 4.80−4.89 (m, 2H, 3′ and 2′), 5.75 (br s, 1H, 1′), 6.28 (br s, 1H,5), 7.63 (br s, 1H, 6), 8.59 (br s, 1H, NH), 9.16 (br s, 1H, NH).

*Diethyl(6-(4-(hydroxyamino)-2-oxopyrimidin-1(2H)-yl)-2,2-dimethyltetrahydrofuro[3,4-d][1,3]dioxol-4-yl)methyl Phosphate (**26**).* Compound **25** (450 mg, 1.07 mmol) was dissolved in 1 mL of ethanol. Hydroxyl ammonium acetate (pH 6.5, 5N, 2 mL) was added to it, and the mixture was stirred at 37 °C for 17 h. The reaction crude was then purified over silica gel (9% MeOH in DCM). Organic fractions containing the desired compound were mixed together and concentrated to yield compound **26** (45 mg, 9%). ^{1}H NMR ($CDCl_3$) δ 1.30−1.31 (m, 9H, *iso* CH_3 and *diethyl* $2CH_2$), 1.53 (s, 3H, *iso* CH_3), 4.08−4.24 (m, 7H, 5′, 5″, 4′, and *diethyl* $2CH_2$), 4.80 (br m, 1H, 3′), 4.88 (br m, 1H, 2′), 5.68 (br s, 1H, 1′), 6.70 (d, J = 7.36 Hz, 1H, 5), 6.92 (br s, 1H, NH), 7.48 (d, J = 6.52 Hz, 1H, 6).

*(3,4-Dihydroxy-5-(4-(hydroxyamino)-2-oxopyrimidin-1(2H)-yl)-tetrahydrofuran-2-yl)methyl Phosphate (**27**).* Compound **26** (37 mg, 0.08 mmol) was dissolved in 1 mL of anhydrous DCM and cooled to 0 °C. TMSBr (130 mg, 0.84 mmol) was added to the reaction mixture and stirred for 10 min at 0 °C. After additional stirring at room temperature for 30 min, the reaction mixture was concentrated, and 1 mL of water was added to it. The aqueous reaction mixture was then purified over HPLC by reverse phase chromatography (Supporting Information). Aqueous fractions containing compound **27** were lyophilized and neutralized by NH_4OH to yield the ammonium salt of the target compound **27** (10 mg, 33%). ^{1}H NMR (D_2O) δ 3.93 (br, m, 2H, 5′ and 5″), 4.18 (m, 1H, 4′), 4.29 (dd, J = 2.84, 2.30 Hz, 1H, 3′), 4.36 (dd, J = 5.60, 6.12 Hz, 1H, 2′), 5.80 (d, J = 8.24 Hz, 1H, 5), 5.92 (d, J = 6.44 Hz, 1H, 1′), 7.26 (d, J = 8.08 Hz, 1H, 6). ^{31}P (D_2O) δ 3.39. ESI (−) m/z calcd for $C_9H_{14}N_3O_9P$[M − H^+] 339.05, found 338.21 Da.

Enzymology. ODCases from *Methanobacterium thermoautotrophicum* (*Mt*), *Plasmodium falciparum* (*Pf*), and *Homo sapiens* (*Hs*) were cloned, expressed, and purified, as described earlier.[4,12] Enzyme activity measurements were performed at 55 °C (*Mt*ODCase) and 37 °C (*Pf*- and *Hs*ODCases) on the isothermal titration calorimeter (VP-ITC, MicroCal, Northampton, MA) as described previously.[13]

Enzyme Inhibition. The inhibition of ODCase from different species by compounds **14** and **27** was evaluated by the competitive inhibition method.[13] Enzyme stock samples were prepared in assay buffer (50 mM Tris, 40 mM NaCl, and 20 mM DTT) and incubated overnight at room temperature. Assay samples were prepared in 50 mM Tris, 20 mM DTT buffer, pH 7.5. Small aliquots of enzyme stock were diluted into assay buffer to give a final enzyme concentration of 20 nM (*Mt*), 60 nM (*Hs*), and 60 nM (*Pf*). Control reactions, without inhibitor, were initiated by a single injection of **2**. The final substrate concentration was 40 μM (*Mt*), 20 μM (*Hs*), and 12 μM (*Pf*). The final assay concentrations of compound **14** were as follows: for *Mt*ODCase, 0, 15, 30, 50, and 100 μM; for *Hs*ODCase, 0, 25, 50, 100, and 150 μM; for *Pf*ODCase, 0, 25, 50, and 100 μM. The concentrations of compound **27** in the assay sample were 0, 25, 50, 100, and 150 μM for the *Hs*ODCase. In the competitive inhibition assay of compounds **14** and **27**, the reaction was initiated by addition of the substrate **2** to the mixture of enzyme and inhibitor. Reactions were performed in triplicate.

Data Analysis. The raw kinetic data obtained from isothermal titration calorimetry (ITC) experiments were analyzed using the Origin 7.0 program. Raw and analyzed kinetic data sets of inhibitor **14** with *Mt*ODCase are provided in Figure 1. The reaction progress

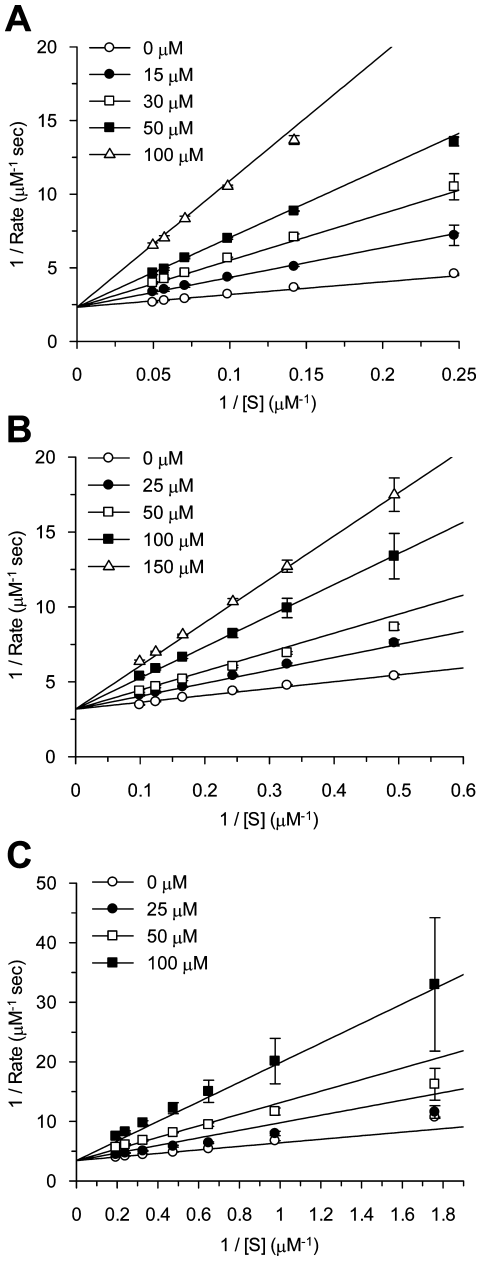

Figure 1. Double-reciprocal plots for compound **14** against *Mt*- (A), *Hs*- (B), and *Pf*ODCases (C).

curves obtained from the ITC experiment at various concentrations of inhibitor (raw data) are represented in Figure 1A. The inhibition constant (K_i) was derived by converting the raw data from inhibited reactions to Michaelis−Menten curves (Figure 1B) by use of the Substrate Only mode in the Origin software to fit the raw data. From this typical rate versus substrate concentration, [S], plot, reaction rate at each substrate concentration in the absence and presence of the inhibitor could be computed. The data from inhibition assays were plotted using the double reciprocal plots (1/rate vs 1/[S]) at various concentrations of inhibitor to confirm that the inhibition is competitive in nature (Figure 1C). For a detailed description of the data analysis, please refer to ref 13.

Crystallographic Analyses. All *Hs*ODCase concentrations were determined using a BioRAD protein assay kit and BSA as a standard. ODCase protein was dissolved in 20 mM Tris (pH 8.0), 10 mM NaCl. *Hs*ODCase complex crystals were grown in hanging drops using 1.6–1.7 M ammonium sulfate, pH 7.0–9.0, as the precipitant. All crystals grew in space group $P2_1$, with unit cell dimensions deviating less than 1% from a = 69.8 Å, b = 61.6 Å, c = 71.4 Å, and β = 112.5°. For data collection, the crystals were cryoprotected by 25% glycerol or Parotone-N oil before flash-freezing in a stream of boiling nitrogen. Diffraction data for the crystals of *Hs*ODCase cocrystallized with compound **27** were collected at 100 K and λ = 0.979 490 Å on beamline 08ID-1 at the Canadian Macromolecular Crystallography Facility, Canadian Light Source, Inc.[15] All data were reduced and scaled using XDS.[16] The diffraction data for *Hs*ODCase cocrystallized with compound **14** were collected at 100 K and λ = 1.541 79 Å in-house on a Rigaku 007 rotating anode equipped with multilayer optics and a MAR345 IP area detector. Data were reduced and scaled using HKL2000.[17] Data collection and refinement statistics for all data sets are given in Table S3 (Supporting Information). The structures of all complexes were determined using molecular replacement techniques with the help of the program package MOLPREP;[18] subsequent refinements were done with Refmac-5.5[19] and model building using COOT.[20] Atomic coordinates and structure factors have been deposited into the Protein Data Bank (PDB IDs: 4HIB and 4HKP).

***In Vitro* Parasitology.** Human malaria parasites were grown in O blood obtained by venipuncture of volunteers. Cultures of the laboratory line *ItG* were maintained by the method of Trager and Jensen[21] using RPMI 1640 supplemented with 10% human serum and 50 μM hypoxanthine. *In vitro* viability assays were performed using the SYBR Green method.[22] Briefly, the compound was dissolved in RPMI 1640 to a final concentration of 10 mg/mL and was then sterilized by passing it through a 0.22 μM filter. The compound was then serially diluted across a 96 well plate (concentrations up to 500 μg/mL) containing a constant number of parasites per well, with the final wells in the series receiving no compound. After 48 h in an atmosphere of 3% CO_2, 2% O_2, and 95% N_2, the growth of the parasites in individual wells was determined by adding 100 μL of a solution containing 2 μL of SYBR Green stock solution in 11 mL of a solution containing buffer and Triton X-100. The relative fluorescence was determined using a GMG fluorescent plate reader and was compared with the results obtained with a chloroquine control. Assays were done in quadruplicate. The concentration of compound that inhibited the growth of 50% of the cultures (IC_{50} values) was determined using a nonlinear regression analysis of the dose–response curve using the following equation:

$$\text{Abs} = N_{max}(1 - ([I]/([I] + IC_{50}))) + \text{Bkg}$$

where the experimentally observed absorption (Abs) is fit to the inhibitor concentrations, [I]. Sigma Plot 2000 (Jandel Scientific) was then used to best-fit and determine the observed values for completely dead parasites (Bkg), the difference between Bkg and completely alive parasites (N_{max}, i.e., when no inhibitor is present), and the 50% value (IC_{50}) between Bkg and N_{max}.

RESULTS AND DISCUSSION

In our earlier study, we reported the plasticity of the ODCase catalytic site toward purine and pyrimidine nucleotide ligands and discussed their unusual mode of binding.[9,12] CMP, a pyrimidine nucleotide, is a weak inhibitor of ODCase with a K_i of 1200 ± 700 and 1400 ± 100 μM against *Mt*- and *Hs*ODCases, respectively (Table 1). K_i values were determined in ITC-based enzymatic assays as reported in earlier work (Figure 1).[13] Structurally, the main difference between CMP and **1** is an amino moiety replacing the ketone moiety at the C4 position of CMP. Regardless of its close similarity to **1**, CMP binds to ODCase in an unusual position, retaining its low-energy conformation, with its nucleobase projecting away from the active site. The ribose ring adopts the 3′-*endo* conformation and the base is oriented *anti* to the ribose ring.[11,12]

Table 1. Inhibition Parameters (K_i) for Nucleotide Ligands against ODCases from *Mt*, *Hs*, and *Pf*

	ODCase inhibition, K_i (μM)		
Ligand	*Mt*	*Hs*	*Pf*
1	330 ± 10	220 ± 100	210 ± 10
CMP	1200 ± 700	1400 ± 100	>10000
14	11.1 ± 0.4	28.3 ± 1.5	22.1 ± 3.2
27			>1000

In the case of uracil-based nucleotide ligands, the backbone -NH- of Ser127 in the binding pocket of ODCase interacts with the O4 atom of the uracil ring while the Ser127 side chain −OH serves as a hydrogen bond acceptor to the N3 proton. Earlier structural studies by Wu et al. with the S127A ODCase mutant showed that the hydrogen bonds with the side chain of Ser127 residue are important for the correct placement of the uracil ring in the active site.[23] In the case of CMP, the phosphate and ribosyl moieties are held in place by similar hydrogen bonding patterns to the one observed with **1**. The cytosine base, however, adopts an *anti* instead of a *syn* conformation. In this conformation the cytosine moiety is pointing away from the Ser127 residue. Even if the cytosine position were more favorable, the tertiary N3 could not act as hydrogen bond donor to Ser127 nor is there any other suitable atom to form a hydrogen bond interaction with backbone atoms, as was seen in the case of **1** (Figure 2 and 3C).

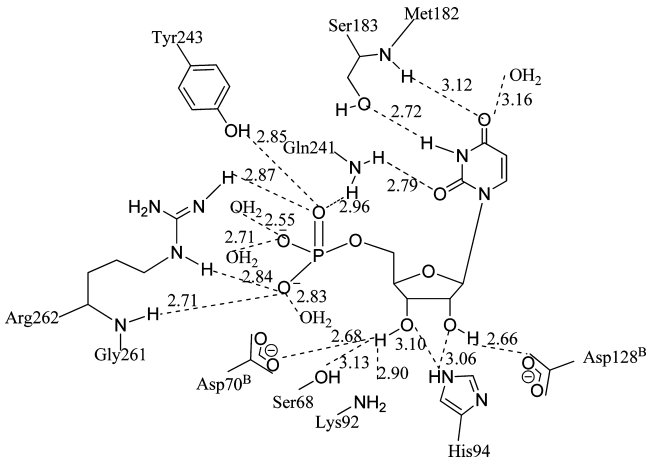

Figure 2. Hydrogen bonding interactions between **1** and the various active site residues of *Hs*ODCase.

Therefore, we envisioned that modification of the N3 and N4 positions of CMP with oxygen may improve its potential to interact within the active site and increase its affinity for ODCase. Thus, the synthesis of compounds **14** and **27** was attempted.

These compounds could be synthesized from either cytidine or CMP. The basic tertiary nitrogen of cytidine (p*K*a 4.2)[24] and CMP (p*K*a 5.6)[24] was oxidized with *meta*-chloroperbenzoic acid (*m*-CPBA) to yield cytidine-N^3-oxide (Cyd-N^3-oxide, **13**) and CMP-N^3-oxide (**14**), respectively (Scheme 1).[25] N^4-hydroxy-cytidine (N^4-OH-Cyd, **15**) was obtained by reacting cytidine with hydroxyl ammonium acetate (pH 6.5). Synthesis of N^4-OH-CMP (**27**) required the protection of the 2′- and 3′-hydroxyl moieties of cytidine with isopropylidene and the 5′-

dx.doi.org/10.1021/jm301176r | J. Med. Chem. 2012, 55, 9988–9997

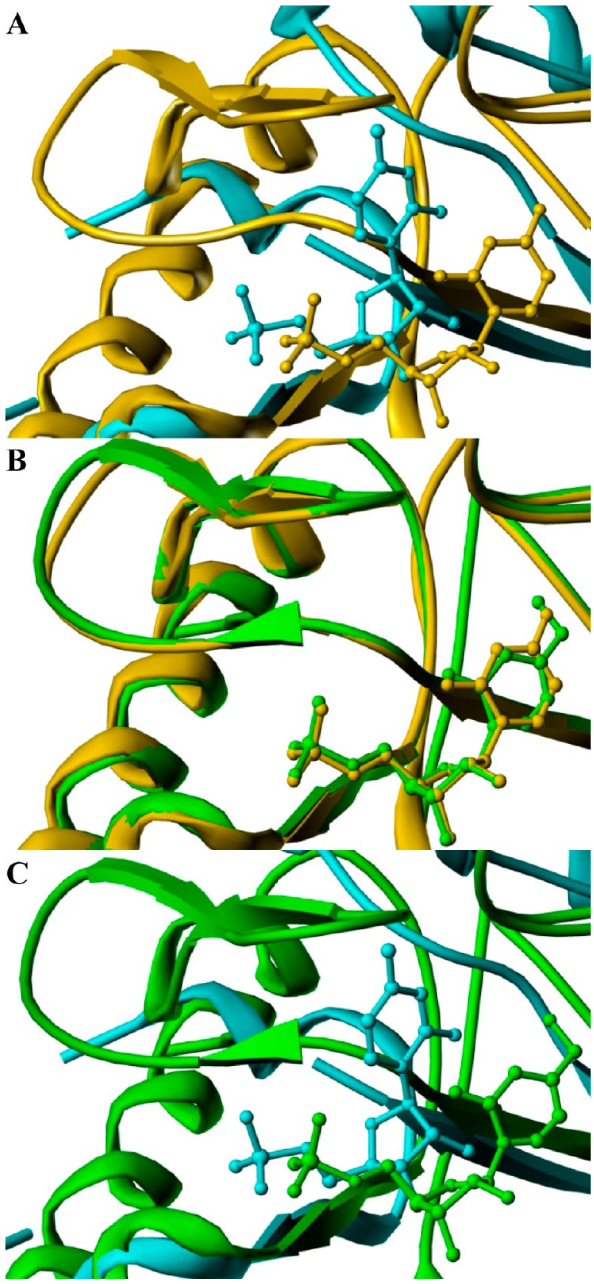

Figure 3. Comparison of the bound conformations of **1**, CMP, and compound **27** in ODCase active site. (A) *Hs*ODCase bound by **1** (yellow) superimposed onto *Mt*ODCase complexed with CMP (cyan); (B) *Hs*ODCase bound by **1** (yellow) superimposed onto *Hs*ODCase bound to N^4-OH-CMP (**27**) (green); (C) *Mt*ODCase with CMP (cyan) superimposed onto *Hs*ODCase bound to **27** (green).

hydroxyl moiety with diethyl chlorophosphate followed by treatment with hydroxyl ammonium acetate at pH 6.5. All protecting groups were removed by trimethylsilyl bromide (TMSBr) to yield the desired compound **27** (Scheme 2). Compounds **13**, **14**, **15**, and **27** were characterized confirming the structures unambiguously as the desired cytidine and CMP derivatives by infrared spectroscopy (Figures S1−S4, Supporting Information), and ^{1}H NMR spectroscopy (Figure 4, and Figures S5−S8, Supporting Information). Additionally, chemical analyses using the classical ferric chloride test were employed to characterize the oxidation at N3 vs N4 position

Scheme 1. Synthesis of Cytidine Derivatives[a]

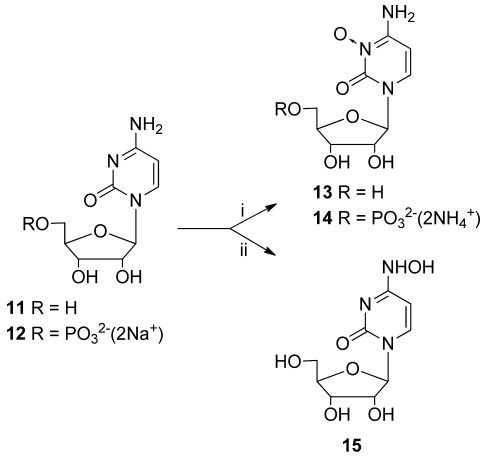

[a]Reagents and conditions: (i) *m*-CPBA, methanol, rt; (ii) 5 N hydroxyl ammonium acetate, pH 6.5, 35 °C.

Scheme 2. Synthesis of Compound 27[a]

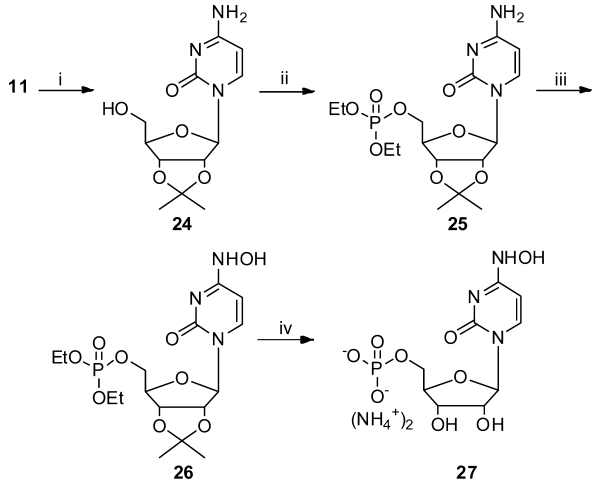

[a]Reagents and conditions: (i) acetone/H$^+$, rt; (ii) diethylchlorophosphate, py, 0 °C to rt; (iii) 5 N hydroxyl ammonium acetate, 35 °C, 13 h; (iv) TMSBr, DCM, 0 °C to rt.

on CMP.[26−28] For the compounds oxidized at the N3 position (**13** and **14**), an orange-red color was observed, whereas for the N4-oxidized cytidine derivatives **15** and **27**, a blue color was observed (Figure 5). The interactions between the mononucleotide derivatives **14** and **27**, and ODCase were investigated, and the nucleoside derivatives **13** and **15** were evaluated in cell-based assays.

CMP-N^3-oxide (**14**) inhibited *Mt*-, *Hs*-, and *Pf*ODCases reversibly with K_i values of 11.1 ± 0.4, 28.3 ± 1.5, and 22.1 ± 3.2 μM, respectively (Table 1). Compared with CMP, compound **14** showed a 100-fold increase in ODCase inhibition. Compound **27**, which is a derivative of CMP at the N4 position, did not display significant inhibition of *Pf*ODCase up to a concentration of 1 mM of the inhibitor.

Antiplasmodial activities against *P. falciparum* of nucleosides **13** and **15** (nucleoside forms of **14** and **27**, respectively) were determined by a fluorescence-based SYBR-green assay. Inhibitory concentrations (IC_{50}) for compounds **13** and **15** were 411 ± 22 and 610 ± 38 μg/mL against *P. falciparum* ItG, respectively. Compound **13** showed better potency than the

dx.doi.org/10.1021/jm301176r | *J. Med. Chem.* 2012, 55, 9988−9997

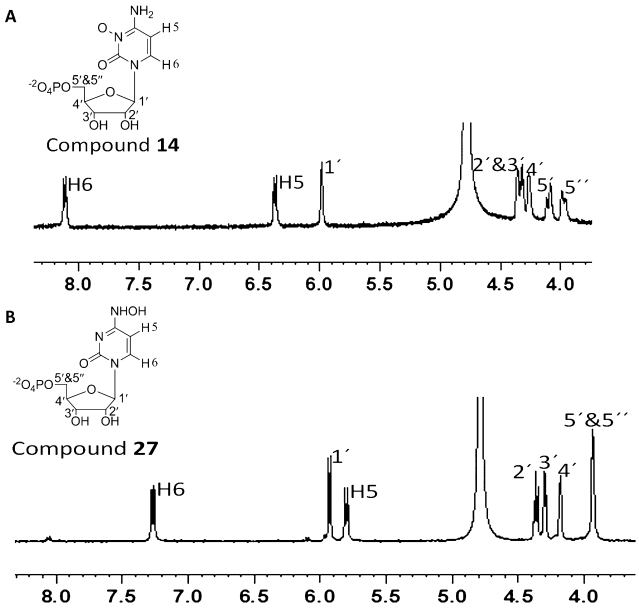

Figure 4. ^{1}H NMR spectra for compounds **14** (A) and **27** (B).

N^4-hydroxy derivative **15**, a trend that correlates with the weaker enzymatic inhibition by the nucleotide derivative **27**. *In vitro* cellular activities of these cytidine nucleosides are also a reflection of the fact that these compounds have entered the cell and were phosphorylated by a kinase in order to inhibit the target enzyme, ODCase.

CMP-N^3-oxide (**14**) and N^4-OH-CMP (**27**) were cocrystallized with *Hs*ODCase to investigate the influence of N^3-oxide and N^4-hydroxy substitutions, respectively, on the ligand orientations and their interactions in the ODCase active site. These cocrystal structures revealed very interesting outcomes. In the X-ray crystal structure of compound **14** bound to *Hs*ODCase, migration of oxygen was observed from N3 to N4, as well as to the C5 position (Figure 6). Compound **27** was bound to *Hs*ODCase in both *cis* and *trans* conformations exhibiting an orientation and conformation similar to that with **1** in the ODCase active site (Figure 7).

Crystals of compound **14** with ODCase proved to be difficult to grow in comparison to cocrystals with other pyrimidine derivatives in our laboratory. In the electron density map from the cocrystal with **14**, the pyrimidine portion exhibited changes in the atomic arrangement. The oxygen atom migrated from N3 to N4 or the C5 position of the cytosine ring (Figure 6A,C,D). These rearranged or modified nucleotides, presumably during the crystallization process, were each bound to ODCase in a 2′-*endo*,*syn* conformation. The binding orientations of these two rearranged products in the active site of ODCase and the corresponding interactions with the active site residues are similar. In fact, the orientation and the binding site interactions of the rearranged products are also similar to the ones observed in the cocrystal structure of **1** with human ODCase. This is indeed a surprising outcome since CMP itself binds in atypical fashion in the binding site of ODCase in comparison to other pyrimidine nucleotides (Figures 2, 3, and 6E,F).

The rearranged ligand N^4-OH-CMP from compound **14** engaged in three hydrogen bond interactions with Ser183, one with the backbone −NH−, one with the side chain hydroxyl moiety, and a third one with a tightly bound water molecule (H_2O637) in the ODCase active site (Figure 6E). The second rearranged ligand, 5-OH-CMP from compound **14**, formed two hydrogen bonds: one between N3 of the ligand and the side chain of Ser183 and the other between the 4-amino moiety and the same water molecule H_2O637 (Figure 6F).

It was indeed intriguing to observe these unusual products N^4-OH-CMP and 5-OH-CMP, when CMP-N^3-oxide (**14**) was incubated with *Hs*ODCase. However, our laboratories have observed such unusual and unexpected behavior for various ligands in the presence of ODCase, for example, with 6-cyano-UMP (**4**), 6-iodo-UMP (**6**), 6-azido-UMP (**5**), and others.[29−31] Interestingly, pyrimidine-*N*-oxides are known to undergo Dimroth rearrangements, a classical mechanism where endocyclic and exocyclic nitrogens switch places.[28,32] In fact, the Dimroth rearrangement, also known as amidine rearrangement, was reported on cytidine-N^3-oxide (**13**) under alkaline conditions.[33] Presumably, if one were to accept the idea that a Dimroth rearrangement occurred in the binding site of ODCase after the binding of compound **14**, Figure 6G outlines a plausible mechanism. According to this, the electron-withdrawing nature of the N3-oxide of **14** weakens the C2−N3 bond (Figure 6G, species **II**), and the labile C2−N3 bond yields to the acyclic reactive isocyanate species **III** with the participation of the lone pair of electrons (Figure 6G). Subsequently, a 180° rotation around the C4−C5 bond followed by the ring closure via species **IV** leads to the N^4-OH-CMP product, observed as one of the two products bound in the active site of ODCase. Alternately, species **III** could undergo tautomerization yielding species **VI**, which then sets the stage for a totally different outcome. Species **VI**, after a 180° rotation of the N3−C4 and C4−C5 bonds, yields species **VII**. This species could lead to the oxazete-like species **VIII**. Oxazetes are relatively stable entities that could even be isolated with appropriate stabilizing groups.[34,35] Further, N3−C2 ring closure and deprotonation at C5 position followed by rearrangement of the electrons leads to species **IX**. Collapse

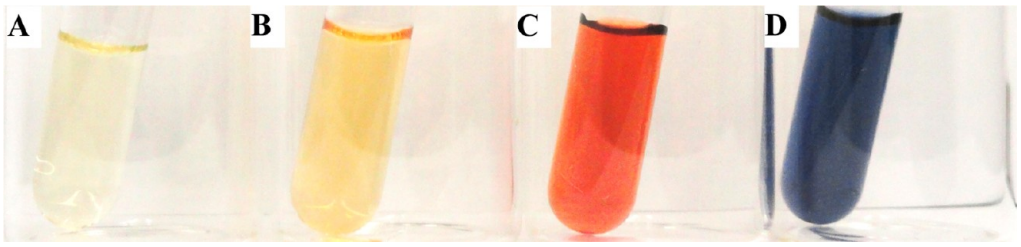

Figure 5. Ferric chloride color test for (A) deionized water alone, (B) CMP, (C) compound **14**, and (D) compound **27**. Deionized water and CMP were used as control experiments (panels A and B). N^3-Oxidized compounds **13** and **14** produced the characteristic red-orange color as shown in panel C. N^4-Oxidized compounds **15** and **27** produced deep blue color, as shown in panel D.

dx.doi.org/10.1021/jm301176r | *J. Med. Chem.* 2012, 55, 9988−9997

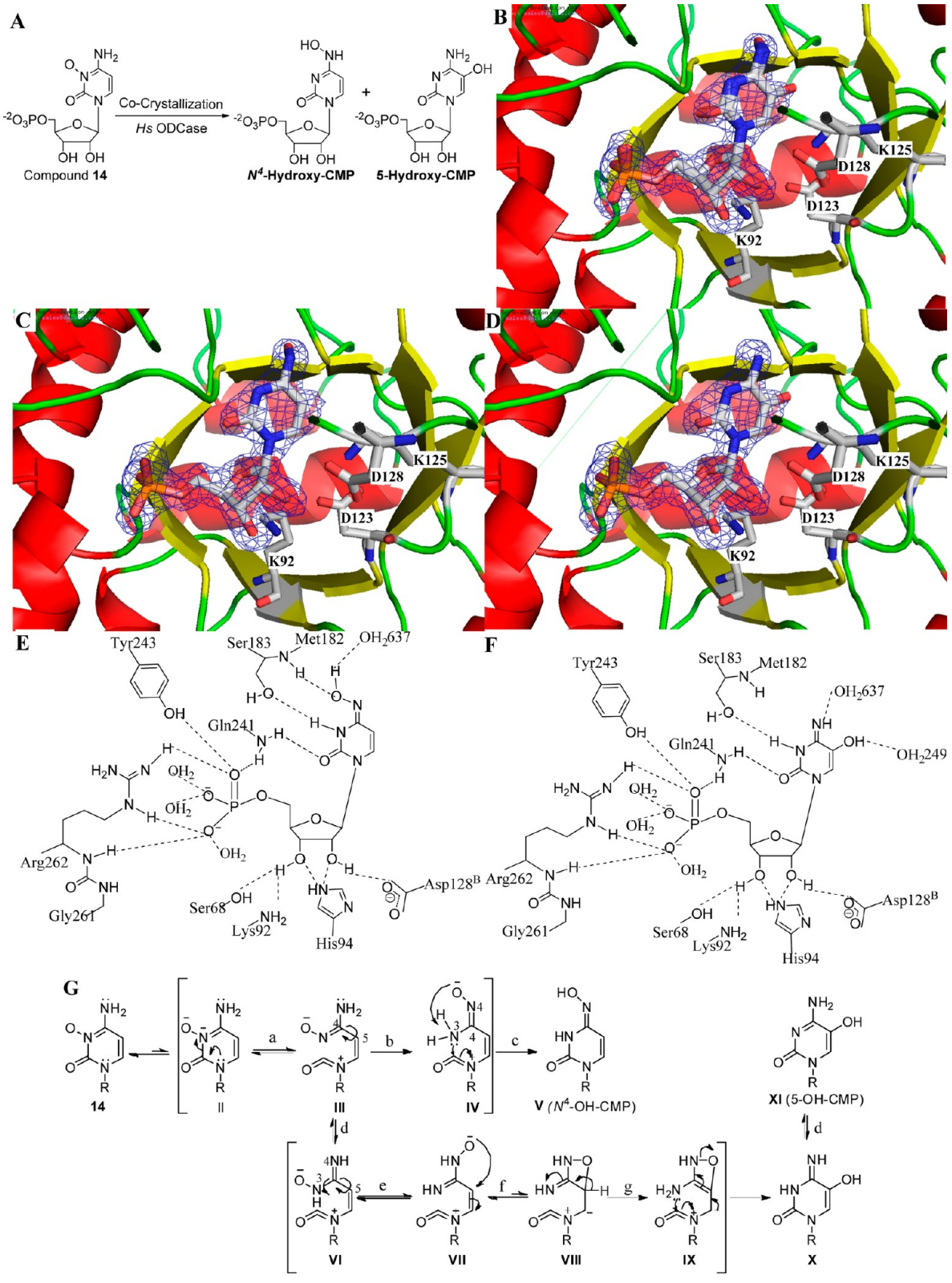

Figure 6. X-ray crystal structure of the complex generated by incubating ODCase with compound **14**. Panel A shows the rearranged products, N^4-OH-CMP and 5-OH-CMP, generated from **14** during cocrystallization with *Hs*ODCase. Panel B shows the electron density map and the resulting products fit into the observed electron density for the rearranged products N^4-OH-CMP and 5-OH-CMP when **14** and *Hs*ODCase were cocrystallized. Panels C and D show the products N^4-OH-CMP and 5-OH-CMP bound in the active site of *Hs*ODCase separately as stick models to the experimental electron density map ($2F_o - F_c$) displayed at a 1σ value. *Hs*ODCase is presented as a cartoon model and colored with respect to its secondary structure (α-helix, red; β-sheet, yellow; loop, green). Catalytic residues of K92, D123, K125, and D128 from *Hs*ODCase are also shown as capped-stick models. Panels E and F illustrate the hydrogen bonding networks between the various active site residues of *Hs*ODCase and the rearranged products N^4-OH-CMP and 5-OH-CMP, respectively. Panel G shows a plausible rearrangement mechanism for ligand **14** to yield N^4-OH-CMP and 5-OH-CMP: (a) ring-opening at C2−N3, (b) 180° rotation about C4−C5 bond leads to formation of the *Z*-isomer, species **IV**, (c) ring

dx.doi.org/10.1021/jm301176r | J. Med. Chem. 2012, 55, 9988−9997

Figure 6. continued

closing due to the intramolecular proton extraction by N-oxide from the amino moiety leading to species **V**, one of the two products identified in the cocrystal structure, (d) amine−imine (N3 and N4) tautomerization, (e) first, rotation around C4−C5, followed by torsional rotation about C4−N3 leads to the *E*-isomer leading to species **VII**, (f) nucleophilic attachment of hydroxylamine onto C5 to yield species **VIII**, (g) deprotonation at C5 and followed by rearrangement of electrons to generate ene−amine species **IX**, then ring closure at C2−N3, followed by regeneration of the C5−C6 double bond and the migration of the oxygen from N4 to C5 leading to iminohydroxy species **X**, or its tautomer **XI**, the second product observed in the binding site of ODCase cocrystallized with CMP-N^3-oxide (**14**).

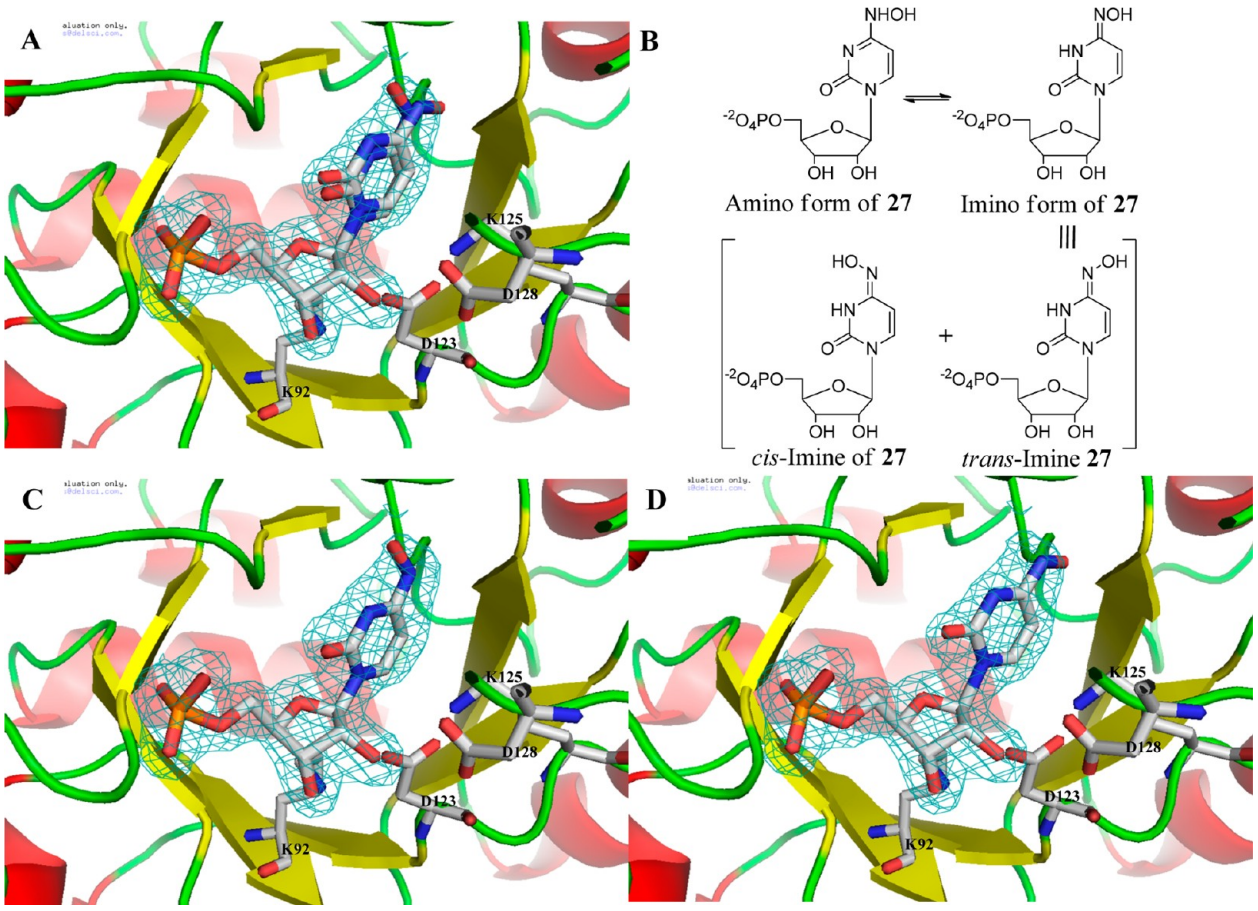

Figure 7. X-ray crystal structure of the complex generated by incubating *Hs*ODCase with compound **27**. (A) Active site region of the *Hs*ODCase with ligand **27** bound in different conformations. (B) Amino−imino tautomers of **27** and the *cis*−*trans* imino isomers of the exocyclic N^4-OH moiety with respect to the N3 of the pyrimidine. Panels C and D present compound **27** bound in the *cis*- and *trans*-conformation, respectively, in the active site of *Hs*ODCase. The enzyme is presented as a cartoon model, colored with respect to the secondary structure (α-helix, red; β-sheet, yellow; loop, green). Compound **27** is shown in capped stick representation and the electron density map ($2F_o - F_c$) is rendered at a value of 1σ. Catalytic residues K92, D123, K125, and D128 of *Hs*ODCase are shown as stick models.

of the C6 anion to generate C5−C6 double bond and subsequent rearrangement leads to the formation of **X** with a C5-OH moiety. Compounds **X** and **XI** are the amine−imine tautomeric forms for 5-OH-CMP, and the latter species **XI** was observed in the catalytic site of ODCase as the second product when incubated with CMP-N^3-oxide (**14**). While there is no proof that these complex rearrangements could happen in the binding site of ODCase, the mechanism described above provides a plausible explanation for what is observed when ODCase is incubated with CMP-N^3-oxide (**14**). However, ODCase was known for inducing unusual and energetically demanding ligand transformations that would not happen without the enzyme.[29,30]

In order to rule out the possibility that the crystallization buffer (Tris or HEPES) played any role in initiating or accelerating the rearrangement of **14**, we conducted UV spectrophotometric studies on compound **14**. Thus, compound **14** was incubated with crystallization buffer, devoid of ODCase. UV spectra were recorded for up to 24 h, the average time it takes to generate crystals from the protein solution. There was no change observed in the UV profiles of **14** even after this prolonged exposure (Table S2 in Supporting Information). This suggests that the rearrangement of **14** probably took place during the cocrystallization process and presumably in the active site of the enzyme itself.

In the complex of compound **27** (N^4-OH-CMP) bound to the active site of *Hs*ODCase, the nucleobase assumed a *syn*- and the ribosyl moiety a 2′-*endo*-conformation. The 5′-*O*-phosphate moiety of compound **27** maintained strong hydrogen bond interactions with Gly261 and Arg262 and with three crystallographic water molecules H_2O2, -3, and -33. In fact, the conformation of **27** in the active site of ODCase is similar to

dx.doi.org/10.1021/jm301176r | *J. Med. Chem.* 2012, 55, 9988−9997

that observed with **1** (Figure 3B).[36] Compound **27** could exist in two tautomeric forms, where the N4 group could assume sp^2 or sp^3 hybridization, resulting in an imino or amino moiety, respectively (Figure 7B). In an aqueous environment, it was reported that the imino tautomer is more predominant, and the dipole moment of the imino tautomer of N^4-OH cytosine is close to that of uracil.[37,38] Thus, it is conceivable that **27** binds to the ODCase active site with a conformation similar to that of **1**.

Based on the cocrystal structure of **27** bound to ODCase, the imino tautomer of **27** could exist in both *cis* and *trans* conformations with respect to N3 (Figure 7A). In the *cis* conformation of **27** (Figure 7C), the hydroxyl group at the N4 position formed a hydrogen bond (2.3 Å) with the −NH group of Ser183. While **27** is in the *trans* conformation (Figure 7D), the hydroxyl of Ser183 forms a hydrogen bond with N3 of the pyrimidine ring (2.7 Å). Interestingly, both of these interactions are observed when **1** is bound in the active site of ODCase.[11] Interactions of **27** with Ser183 are important for locking the nucleobase in the *syn* conformation. An earlier study by Wu et al. also showed that in the complex of the ODCase mutant S127A with 6-aza UMP (**9**) the interactions between the Ser127 residue and the uracil moiety are determining factors for the binding of the ligand in the *syn* conformation.[23]

In summary, CMP and **1**, pyrimidine mononucleotides that differ at one key functional group: an amino vs keto moiety at the C4 position, interact with ODCase quite distinctly. The introduction of the oxygen atom at the N3 position of CMP led to a 100-fold increase in ODCase inhibition, 10-fold better than even the product **1**. A potential rearrangement in the binding site of ODCase could contribute to the observed products, when cocrystallized with the N^3-oxide derivative. On the other hand, when the oxygen atom was introduced in the form of an N^4-hydroxyl substitution on CMP, binding interactions of the CMP derivative are similar to those with **1** in the active site of ODCase. Because these results indicate that N-hydroxylated cytidine derivatives behave significantly differently from their parent compound, showing improved potency against ODCase, the nucleoside versions of these CMP-based nucleotides could lead to a new class of therapeutic agents.

■ ASSOCIATED CONTENT

Supporting Information

Purity and spectrometric data. This material is available free of charge via the Internet at http://pubs.acs.org.

■ AUTHOR INFORMATION

Corresponding Author

*Mailing address: Center for Molecular Design and Preformulations, University Health Network, #5-356 MaRS/TMDT, 101 College Street, Toronto, ON M5G 1L7, Canada. Tel. (416) 581-7601. E-mail: lkotra@uhnres.utoronto.ca.

Notes

The authors declare no competing financial interest.

■ ACKNOWLEDGMENTS

This work was supported by a grant from the ISTPCanada. Authors thank Dr. Angelica Bello for useful discussions on the molecular mechanisms. E.F.P. acknowledges support through the Canada Research Chairs program. Research described in this paper was in performed in part at the Canadian Light Source, which is supported by the National Sciences and Engineering Research Council, the National Research Council Canada, the Canadian Institutes of Health Research, the Province of Saskatchewan, Western Economic Diversification Canada, and the University of Saskatchewan. This research was funded in part by the Ontario Ministry of Health and Long Term Care. The views expressed do not necessarily reflect those of the OMOHLTC.

■ REFERENCES

(1) Radzicka, A.; Wolfenden, R. A proficient enzyme. *Science* **1995**, *267* (5194), 90−93.

(2) Miller, B. G.; Wolfenden, R. Catalytic proficiency: The unusual case of OMP decarboxylase. *Annu. Rev. Biochem.* **2002**, *71*, 847−885.

(3) Meza-Avina, M. E.; Wei, L.; Buhendwa, M. G.; Poduch, E.; Bello, A. M.; Pai, E. F.; Kotra, L. P. Inhibition of orotidine 5′-monophosphate decarboxylase and its therapeutic potential. *Mini-Rev. Med. Chem.* **2008**, *8* (3), 239−247.

(4) Bello, A. M.; Poduch, E.; Liu, Y.; Wei, L.; Crandall, I.; Wang, X.; Dyanand, C.; Kain, K. C.; Pai, E. F.; Kotra, L. P. Structure−activity relationships of C6-uridine derivatives targeting plasmodia orotidine monophosphate decarboxylase. *J. Med. Chem.* **2008**, *51* (3), 439−448.

(5) Bello, A. M.; Konforte, D.; Poduch, E.; Furlonger, C.; Wei, L.; Liu, Y.; Lewis, M.; Pai, E. F.; Paige, C. J.; Kotra, L. P. Structure−activity relationships of orotidine-5′-monophosphate decarboxylase inhibitors as anticancer agents. *J. Med .Chem.* **2009**, *52* (6), 1648−1658.

(6) Lewis, M.; Meza-Avina, M. E.; Wei, L.; Crandall, I. E.; Bello, A. M.; Poduch, E.; Liu, Y.; Paige, C. J.; Kain, K. C.; Pai, E. F.; Kotra, L. P. Novel interactions of fluorinated nucleotide derivatives targeting orotidine 5′-monophosphate decarboxylase. *J. Med. Chem.* **2011**, *54* (8), 2891−2901.

(7) http://www.rcsb.org. Access Date: 11th December, 2011.

(8) Residue numbers refer to the enzyme from *Methanobacterium thermoautotrophicum*. The superscript "B", as in Asp 75^B, indicates that the residue belongs to B subunit.

(9) Poduch, E.; Wei, L.; Pai, E. F.; Kotra, L. P. Structural diversity and plasticity associated with nucleotides targeting orotidine monophosphate decarboxylase. *J. Med. Chem.* **2008**, *51* (3), 432−438.

(10) Langley, D. B.; Shojaei, M.; Chan, C.; Lok, H. C.; Mackay, J. P.; Traut, T. W.; Guss, J. M.; Christopherson, R. I. Structure and inhibition of orotidine 5′-monophosphate decarboxylase from *Plasmodium falciparum*. *Biochemistry* **2008**, *47* (12), 3842−3854.

(11) Wu, N.; Pai, E. F. Crystallographic studies of native and mutant orotidine-5′-phosphate decarboxylases. *Top. Curr. Chem.* **2004**, *238*, 23−42.

(12) Wu, N.; Gillon, W.; Pai, E. F. Crystal structures of inhibitor complexes reveal an alternate binding mode in orotidine-5′-monophosphate decarboxaylase. *J. Biol. Chem.* **2002**, *277* (31), 28080−28087.

(13) Poduch, E.; Bello, A. M.; Tang, S.; Fujihashi, M.; Pai, E. F.; Kotra, L. P. Design of inhibitors of orotidine monophosphate decarboxylase using bioisosteric replacement and determination of inhibition kinetics. *J. Med. Chem.* **2006**, *49* (16), 4937−4945.

(14) Higuchi, T.; Barnstein, C. H. Hydroxylammonium acetate as carbonyl reagent. *Anal. Chem.* **1956**, *28* (6), 1022−1025.

(15) Grochulski, P.; Fodje, M. N.; Gorin, J.; Labiuk, S. L.; Berg, R. Beamline 08ID-1, the prime beamline of the Canadian Macromolecular Crystallography Facility. *J. Synchrotron Radiat.* **2011**, *18* (4), 681−684.

(16) Kabsch, W. XDS. *Acta Crystallogr.* **2010**, *D66*, 125−132.

(17) Otwinowski, Z.; Minor, W. Processing of X-ray diffraction data collected in oscillation mode. *Methods Enzymol.* **1997**, *276*, 307−326.

(18) Vagin, A.; Teplyakov, A. MOLREP: An automated program for molecular replacement. *J. Appl. Crystallogr.* **1997**, *30*, 1022−1025.

(19) Murshudov, G. N.; Vagin, A. A.; Dodson, E. J. Refinement of macromolecular structures by the maximum-likehood method. *Acta Crystallogr.* **1997**, *D53*, 240−255.

(20) Emsley, P.; Cowtan, K. Model building tools for molecular graphics. *Acta Crystallogr.* **2004**, *D60*, 2126−2132.
(21) Trager, W.; Jensen, J. Human malaria parasites in continuous culture. *Science* **1976**, *193*, 673−675.
(22) Smilkstein, M.; Sriwilaijaroen, N.; Kelly, J. X.; Wilairat, P.; Riscoe, M. Simple and inexpensive fluorescence-based technique for high-throughput antimalarial drug screening. *Antimicrob. Agents Chemother.* **2004**, *48*, 1803−1806.
(23) Wu, N.; Gillon, W.; Pai, E. F. Mapping the active site-ligand interactions of orotidine 5′-monophosphate decarboxylase by crystallography. *Biochemistry* **2002**, *41* (12), 4002−4011.
(24) Chang, C.-C.; Lin, P.-Y.; Chen, Y.-F.; Chang, C.-S.; Kan, L.-S. Direct visualization of the triplex DNA molecular dynamics by the fluorescence resonance energy transfer and atomic force microscopy measurements. *Appl. Phys. Lett.* **2007**, *91*, No. 203901, DOI: 10.1063/1.2809406.
(25) Harnden, M. R.; Brown, A. G.; Hodge, R. A. Oxidation of ribonucleic acids with m-chloroperbenzoic acid. *J. Chem. Soc., Perkin Trans. 1* **1973**, *4*, 333−335.
(26) Romo, J.; Rodríguez-Hahn, L.; Jiménez, M. Synthesis of steroidal pyrimidine N-oxides. *Can. J. Chem.* **1968**, *46*, 2807−2815.
(27) Leung, K. K.; Visser, D. W. A new deoxycytidine analog, 5-hydroxy-2′-deoxycytidine. *Biochem. Med.* **1974**, *9*, 237−243.
(28) Delia, T. J.; Olsen, M. J.; Brown, G. B. Cytosine 3-N-oxide and its rearrangement on acetylation. *J. Org. Chem.* **1965**, *30*, 2766−2768.
(29) Fujihashi, M.; Bello, A. M.; Poduch, E.; Wei, L.; Annedi, S. C.; Pai, E. F.; Kotra, L. P. An unprecedented twist to ODCase catalytic activity. *J. Am. Chem. Soc.* **2005**, *127* (43), 15048−15050.
(30) Fujihashi, M.; Wei, L.; Kotra, L. P.; Pai, E. F. Structural characterization of the molecular events during a slow substrate − product transition in orotidine-5′-monophosphate decarboxylase. *J. Mol. Biol.* **2009**, *387*, 1199−1210.
(31) Bello, A. M.; Poduch, E.; Fujihashi, M.; Amani, M.; Li, Y.; Crandall, I.; Hui, R.; Lee, P. I.; Kain, K. C.; Pai, E. F.; Kotra, L. P. A potent, covalent inhibitor of orotidine 5′-monophosphate decarboxylase with antimalarial activity. *J. Med. Chem.* **2007**, *50* (5), 915−921.
(32) El Ashry, E. S. H.; Nadeem, S.; Shah, M. R.; El Kilany, Y. Recent advances in the Dimroth rearrangement: A valuable tool for the synthesis of heterocycles. *Adv. Heterocycl. Chem.* **2010**, *101*, 161−228.
(33) Sako, M.; Kawada, H. A new and efficient synthetic method for $^{15}N_3$-labeled cytosine nucleosides: Dimroth rearrangement of cytidine N_3-oxides. *J. Org. Chem.* **2004**, *69* (23), 8148−8150.
(34) Corkins, H. G.; Storace, L.; Osgood, E. R. A new route to the 4H-1,2-oxazete ring system by the stereospecific oxidation of (*Z*)-3,3-dimethyl-1,1-*bis*(methylthio)-2-butanone oxime. *Tetrahedron Lett.* **1980**, *21*, 2025−2028.
(35) Wieser, K.; Berndt, A. 4*H*-1,2-Oxazete *N*-oxides from 1,1-di-*tert*-butylallenes. *Angew. Chem., Int. Ed. Engl.* **1975**, *14*, 69−70.
(36) Wittmann, J. G.; Heinrich, D.; Gasow, K.; Frey, A.; Diederichsen, U.; Rudolph, M. G. Structures of the human orotidine-5′-monophosphate decarboxylase support a covalent mechanism and provide a framework for drug design. *Structure* **2008**, *16* (1), 82−92.
(37) Shugar, D.; Kierdaszuk. New light on tautomerism of purines and pyrimidines and its biological and genetic implications. *Proc. Int. Symp. Biomol. Struct. Interact. J. Biosci.* **1985**, *8* (Suppl), 657−668.
(38) Les, A.; Adamowicz, L.; Rode, W. Structure and conformation of N4-hydroxycytosine and N4-hydroxy-5-fluorocytosine. A theoretical ab initio study. *Biochim. Biophys. Acta* **1993**, *1173*, 39−48.